NeuroImage: Clinical 37 (2023) 103344

Contents lists available at ScienceDirect

NeuroImage: Clinical

journal homepage: www.elsevier.com/locate/ynicl

Temporal dynamics of cerebral blood flow during the first year after moderate-severe traumatic brain injury: A longitudinal perfusion MRI study

Naomi L. Gaggi [a,b], Jeffrey B. Ware [c], Sudipto Dolui [c], Daniel Brennan [a,b], Julia Torrellas [a], Ze Wang [d], John Whyte [e], Ramon Diaz-Arrastia [c], Junghoon J. Kim [a,b,*]

[a] City University of New York (CUNY) School of Medicine, Townsend Harris Hall, 160 Convent Avenue, Convent Avenue, New York, NY 10031, United States
[b] City University of New York (CUNY) Graduate Center, 365 5th Avenue, New York, NY 10016, United States
[c] University of Pennsylvania, Perelman School of Medicine, 3400 Civic Center Boulevard, Philadelphia, PA 19104, United States
[d] University of Maryland School of Medicine, 655 W Baltimore St. S, Baltimore, MD 21201, United States
[e] Moss Rehabilitation Research Institute, 50 Township Line Road, Elkins Park, PA 19027, United States

ARTICLE INFO

Keywords:
Cerebral blood flow
Arterial spin labeling
Traumatic brain injury
Cognitive function
Longitudinal
Magnetic resonance imaging

ABSTRACT

Traumatic brain injury (TBI) is associated with alterations in cerebral blood flow (CBF), which may underlie functional disability and precipitate TBI-induced neurodegeneration. Although it is known that chronic moderate-severe TBI (msTBI) causes decreases in CBF, the temporal dynamics during the early chronic phase of TBI remain unknown. Using arterial spin labeled (ASL) perfusion magnetic resonance imaging (MRI), we examined longitudinal CBF changes in 29 patients with msTBI at 3, 6, and 12 months post-injury in comparison to 35 demographically-matched healthy controls (HC). We investigated the difference between the two groups and the within-subject time effect in the TBI patients using whole-brain voxel-wise analysis. Mean CBF in gray matter (GM) was lower in the TBI group compared to HC at 6 and 12 months post-injury. Within the TBI group, we identified widespread regional decreases in CBF from 3 to 6 months post-injury. In contrast, there were no regions with decreasing CBF from 6 to 12 months post-injury, indicating stabilization of hypoperfusion. There was instead a small area of increase in CBF observed in the right precuneus. These CBF changes were not accompanied by cortical atrophy. The change in CBF was correlated with change in executive function from 3 to 6 months post-injury in TBI patients, suggesting functional relevance of CBF measures. Understanding the time course of TBI-induced hypoperfusion and its relationship with cognitive improvement could provide an optimal treatment window to benefit long-term outcome.

1. Introduction

Microvascular injury is one of the many neuropathological consequences of traumatic brain injury (TBI). (Morales et al., 2005) Microvascular injury following TBI is a very common and chronic, yet relatively understudied phenomenon. (Sandsmark et al., 2019; Kenney et al., 2016) Animal and pathological studies widely implicate microvascular injury in TBI across the severity spectrum (e.g., Sandsmark et al., 2019; Kenney et al., 2016; DeWitt and Prough, 2003). Microvascular injury demonstrates a relationship with the neurovascular unit that can aid in precipitating secondary damages, such as neurodegeneration. (Sandsmark et al., 2019) Impaired cerebral blood flow (CBF) is a biomarker of microvascular disruption (i.e., traumatic microvascular injury (Kenney et al., 2016) and has clinical importance in TBI because of its relationship with metabolic alterations, (Soustiel et al., 2005) cognitive and functional outcome, (Ware et al., 2020; Kim et al., 2012; Obrist et al., 1979; Hlatky et al., ; Ding et al., 2020) and onset of neurodegenerative diseases. (Chao et al., 2010; Xekardaki et al.,

Abbreviations: TBI, traumatic brain injury; msTBI, moderate-severe traumatic brain injury; CBF, cerebral blood flow; MRI, magnetic resonance imaging; ASL MRI, arterial spin labeled magnetic resonance imaging; EF, executive function; PS, processing speed; VL, verbal learning; FWE, family wise error; GM, gray matter; DisCo-Z, distribution corrected z-score.

* Corresponding author at: City University of New York (CUNY) School of Medicine, Townsend Harris Hall, 160 Convent Avenue, Convent Avenue, New York, NY 10031, United States.

E-mail addresses: ngaggi@ccny.cuny.edu (N.L. Gaggi), Jeffrey.Ware2@pennmedicine.upenn.edu (J.B. Ware), sudiptod@pennmedicine.upenn.edu (S. Dolui), dbrennan@gradcenter.cuny.edu (D. Brennan), jtorrel000@citymail.cuny.edu (J. Torrellas), ze.wang@som.umaryland.edu (Z. Wang), jwhyte@einstein.edu (J. Whyte), Ramon.Diaz-Arrastia@pennmedicine.upenn.edu (R. Diaz-Arrastia), jkim@med.cuny.edu (J.J. Kim).

https://doi.org/10.1016/j.nicl.2023.103344
Received 28 April 2022; Received in revised form 1 February 2023; Accepted 4 February 2023
Available online 11 February 2023

2015; Benedictus, 2017; Ramos-Cejudo et al., 2018; Shively et al., 2012; Wilson et al., 2017; Sweeney et al., 2018) Due to the relationship of CBF with neural health and behavior, understanding the dynamics of CBF alterations after TBI may benefit the implementation of interventions that enhance microvascular function with the ultimate aim of interrupting the progression of further neural and cognitive decline.

CBF in patients with severe TBI has been described longitudinally in the acute post-injury time period (i.e., 0 h to 24 h; (Bouma et al., 1992; Bouma et al., 1991) 0 days to 1 week; (Marion et al., 1991) 0 days to 2 weeks (Martin et al., 1997), with heterogeneity in the direction and extent of CBF change seen amongst TBI patients from days to weeks post-injury. One study, (Inoue et al., 2005) which examined CBF in 20 patients with severe TBI using xenon-enhanced computer tomography, demonstrated persistent decreased CBF between 1 and 6 weeks post-injury, with only a subset of patients returning to a normal CBF level around 3 weeks post-injury. Beyond this time period post-injury, the precise temporal pattern of CBF alterations and variability across patients remains unclear. Determining the temporal pattern of CBF and the amount of variability in CBF change during more chronic time points post-injury in msTBI can shed light on the importance of long-term microvascular injury.

Our group has previously conducted cross-sectional studies using arterial spin labeled (ASL) magnetic resonance imaging (MRI) and confirmed reduced CBF, in widespread brain regions in the chronic phase of moderate-severe TBI (msTBI) as early as 3 months post-injury and as late as 330 months post-injury compared to healthy controls. (Ware et al., 2020; Kim et al., 2010) Post-TBI CBF reductions, measured by MRI and single-photon emission computerized tomography, have previously been demonstrated to persist for years after injury (DeWitt and Prough, 2003; Kim et al., 2010; Stamatakis et al., 2009) and occur in the absence of and independent from visible structural damage. (Kim et al., 2010; Haber, 2018) MRI-based measurements of CBF, specifically ASL MRI, provide an appealing and noninvasive means of assessing microvascular disruption in TBI with high reliability. (Dolui et al., 2016) Advantages of ASL MRI include high spatial resolution, absolute CBF quantification, and lack of exposure to contrast material or ionizing radiation. (Ware et al., 2020) ASL MRI holds clinical utility for assessing perfusion (Telischak et al., 2015; Wilde et al., 2022) and is readily acquired as part of a multimodal MRI examination required to assess heterogeneous TBI-related pathology, accounts for potential structural confounds on perfusion, and allows for the accurate co-registration of perfusion data across patients for quantitative analysis. CBF has become an important biomarker of cognitive function and dysfunction in both aging and neurodegenerative disease, as CBF predicts subsequent cognitive decline (Chao et al., 2010; Xekardaki et al., 2015; Benedictus, 2017) and is associated with pathophysiological changes that overlap with neurodegenerative disorders. (Wilson et al., 2017) Furthermore, microvascular injury-related neurovascular unit dysfunction represents a potentially modifiable target for intervention given its plasticity and responsiveness to pharmacological and vascular-directed therapy. (Sandsmark et al., 2019) Together, this lends itself to the idea that CBF is a promising treatment target for TBI and quantifying CBF may be able to convey important prognostic information in chronic TBI.

However, the time-dependent change of CBF in the chronic phase and its relationship with cognitive recovery is insufficiently characterized. The current study is the first to use multiple follow-up assessments to delineate the pattern on CBF changes during the first year after msTBI to the best of our knowledge. Determining the temporal pattern of CBF and the amount of variability during the first year post-injury in msTBI can shed light on the importance of microvascular injury to cognitive trajectory after TBI and ultimately help in identifying a window of opportunity in which interventions targeted toward microvascular health may be most effective. While we expect to observe decreased CBF based on previous literature demonstrating GM hypoperfusion in chronic msTBI, (Ware et al., 2020; Amyot et al., 2018) understanding the temporal dynamics of CBF during the first year post-injury is an exploratory analysis. In addition, we seek to determine if CBF changes correlate with behavioral changes as we have previously found CBF in TBI at 3 months post-injury to be predictive of cognitive trajectory from 3 to 12 months post-injury. (Ware et al., 2020) Determining the relationship of temporal CBF changes to behavioral improvement and/or decline will support the clinical importance of CBF and help in understanding the ability of CBF to serve as a prognostic and predictive biomarker of microvascular health in chronic TBI. There is no previous longitudinal evidence that incorporates these phases post-injury in msTBI or examines individual specific differences in perfusion. In this study, we employed ASL MRI to quantitatively measure whole-brain and regional CBF in msTBI patients at 3, 6, and 12 months post-injury to determine 1) the temporal dynamics of CBF (i.e., change in CBF between each time point) in patients with TBI during the first year post-injury, and 2) the relationship between longitudinal CBF and cognitive changes.

2. Methods

2.1. Study Population

This study was approved by the Institutional Review Board of the Moss Rehabilitation Research Institute and written informed consent was obtained from the participants or their legally authorized representatives. Patients with moderate-severe TBI were recruited from the outpatient clinical programs at the Drucker Brain Injury Center of the MossRehab Hospital in Philadelphia from 2012 to 2016.

Participants were selected to include those with evidence of injury mechanism consistent with diffuse axonal injury (e.g., immediate loss of consciousness, post-traumatic amnesia, and high-impact closed-head injury). Inclusion criteria for TBI group participation included: (1) an age range of 18 to 64 years old and (2) a history of non-penetrating TBI of at least moderate severity. Severity was defined by either (1) documented loss of consciousness for $\geq$ 12 h; (2) duration of post-traumatic amnesia $\geq$ 24 h; or (3) the Glasgow Coma Scale $<$ 13 from the Emergency Department (not due to sedation, paralysis, or intoxication). Exclusion criteria for participation included: (1) history of prior TBI, central nervous system disease, seizure disorder, schizophrenia, and/or bipolar disorder; (2) history of alcohol or stimulant abuse; (3) inability to complete MRI scanning due to ferromagnetic implants, claustrophobia, or restlessness; (4) pregnancy; (5) non-fluency in English; and/or (6) level of disability too great to allow for completion of testing and scanning 3, 6, and 12 months post-TBI. Participants were also excluded if the total estimated volume of focal intraparenchymal lesions was greater than 5 cm^3 for subcortical lesions and 50 cm^3 for cortical lesions from initial CT/MRI scans.

In total, 42 TBI subjects met the inclusion criteria for this study. 29 participants (age: 32 $\pm$ 13.14 years, 10 female) completed the neuroimaging study at 3, 6, and 12 months post-injury and were considered for the study. So, 29 patients out of 42 both completed all scans and neuropsychological battery tests (detailed below) and passed data quality checks. There were 9 patients who couldn't complete their 6 months follow-up and 4 patients who could not be followed up at 12 months post-injury. The reasons included incarceration, medical complications requiring additional surgery, and voluntary withdrawal. These patients were excluded from the current study. The participants included in this study are a sub-cohort from our previous study. (Ware et al., 2020) In addition, 35 demographically matched HC (mean age = 35 $\pm$ 10.24 years, 9 female) were enrolled and scanned once for this study. The control participants were drawn from acquaintances of study participants, the MossRehab Rehabilitation Research Registry and public notices including IRB approved flyers, tent cards and newspaper advertisements. Exclusion criteria for HC were the same as above, with an additional exclusion for any history of TBI resulting in loss of consciousness or alteration of consciousness.

2.2. Clinical and Neuropsychological Measures

Clinical measures included duration of post-traumatic amnesia, acquired prospectively during hospitalization. In addition, clinical measures included Glasgow Coma Scale and days to follow command, which were extracted from medical records. The duration of post-traumatic amnesia was used as an index of TBI severity, defined as the number of days between the TBI and the date of the 1st of 2 scores ≥ 25 on the Orientation Log (Jackson et al., 1998) administered ≤ 72 h apart. For patients who were discharged from rehabilitation care while still in post-traumatic amnesia, their post-traumatic amnesia duration was estimated conservatively at [days between TBI and rehabilitation discharge] + 1.

Longitudinal neuropsychological data were obtained from TBI patients at 3, 6 and 12 months post-injury and included tests of processing speed, executive function, and verbal learning, which are domains frequently impaired in TBI. Cognitive performance was assessed across three domains, including mental processing speed (PS) as indexed by the Processing Speed Index from the Wechsler Adult Intelligence Scale IV (WAIS-IV) and verbal learning (VL) as indexed by the Rey Auditory Verbal Learning Test. In addition, cognitive performance was assessed by executive functioning (EF) as indexed by a composite measure consisting of an average across t scores of the following tests: Letter-Number Sequencing subtest and Digits Backward section of the Digit Span subtest of the Wechsler Memory Scale IV, Controlled Oral Word Association test, test B from Trails-Making Test, and Color Word section of the Color Word Interference Test from the Delis-Kaplan Executive Function System. For more details on these cognitive tests, please refer to our previous publication (Wechsler, 2014; Lezak, 2004; Benton, Hamsher, & Sivan, 1994; Reitan & Wolfson, 1985; Delis, Kaplan, & Kramer, 2001 referenced in (Rabinowitz et al., 2018).

2.3. Magnetic Resonance Imaging Acquisition

Brain MRI examinations were performed on a 3 Tesla MRI scanner (Siemens Trio, Siemens, Erlangen, Germany). ASL data were acquired using a pseudo-continuous ASL sequence. The labeling was performed with a labeling time/post-labeling delay = 1.5/1.5 s at 9 cm below the center of the imaging volume. The images were acquired using *EPI* imaging with TR/TE = 4 s/18 ms, FOV 220 mm, matrix 64x64, voxel size 3.4x3.4x7.2 mm^3, 18 sequential axial slices (thickness 6 mm) with a between-slice gap of 1.2 mm, and 45 label-control image pairs. ASL MRI provides non-invasive quantification of CBF, (Alsop et al., 2015) has been validated with other established molecular imaging modalities for measuring CBF, is the modality of choice to measure CBF in longitudinal and large scale multisite studies requiring repeated acquisitions. (Dolui et al., 2016) In addition, high-resolution T1 weighted magnetization-prepared rapid gradient echo (MPRAGE) images were also obtained at 1 mm isotropic resolution using the following parameters: TR/TE/TI = 1620/3.08/950 ms, flip angle = 15°, 160 contiguous slices of 1 mm thickness, and matrix 256x192.

2.4. Image Processing.

2.4.1. Lesion Masking

Lesion masks were drawn on T1 by a trained observer who manually segmented the lesion area under the supervision of a neurologist with extensive experience in lesion assessment. Lesions masking was derived from the 3 month post-injury time point. Focal lesions included any cystic cavities and other focal regions of abnormal signal in gray matter (GM). The ITK-SNAP software (version 5.2.1; (Ramos-Cejudo et al., 2018; Shively et al., 2012; Yushkevich et al., 2006) was used for 3D-based segmentation. Total lesion volume was calculated using FMRIB Software Library (FSL version 6.0; https://fsl.fmrib.ox.ac.uk/fsl/fslwiki/FslInstallation). (Smith et al., 2004) An overlap map was created to determine the frequency of lesion location amongst TBI patients. This lesion information was compared to regions of reduced CBF and was also utilized in further analyses (Section 2.4.4). Additional information can be found in Supplemental Table 1.

2.4.2. Pre-processing of Magnetic Resonance Imaging Data

Pre-processing of ASL data and CBF quantification were conducted using SPM12 and the ASL toolbox pipeline. (Wang et al., 2008) The processing consisted of realigning the control/label time series by estimating a six-parameter rigid body spatial transformation and thereafter regressing out the spurious motion component caused by the systematic label/control alteration from the motion parameters before applying the transformation to the images. The realigned images were then smoothed using the Gaussian smoothing kernel (FWHM = 6 mm) to reduce noise. CBF was quantified using the single compartment model with parameters as recommended by Alsop et al. (Alsop et al., 2015) The CBF maps were normalized to the MNI space by combining two transforms: co-registration of mean functional image to each subject's structural image and normalization of the structural image to the MNI space and the maps were used for voxel-wise analysis.

2.4.3. Extraction of Cerebral Blood Flow Values

Marsbar (Brett et al., 2002) software (release 0.45) was used to extract mean CBF values from CBF maps. We utilized a GM mask because CBF in WM is generally below the signal-to-noise ratio threshold of ASL MRI and so WM CBF is beyond the scope of this paper. It is an ongoing issue in TBI research, as diffuse white matter disease is likely present and functional measures (i.e., ASL MRI) have poor sensitivity to WM function. A GM mask was created in MNI space by extracting cortical and subcortical GM from the MNI-ICBM template brain (International Consortium from Brain Mapping) (Fonov et al., 2009; Fonov et al., 2011) using both FMIRB's Automated Segmentation Tool (FAST) and FIRST implemented in FSL. (Smith et al., 2004; Patenaude et al., 2011; Zhang et al., 2001) FIRST was used to segment subcortical regions (e.g., caudate, hippocampus, thalamus, putamen, etc.) and FAST was used to segment tissue classes (i.e., GM, WM, CSF). Using 'fslmaths,' (Smith et al., 2004) the GM tissue classification and combined subcortical regions were binarized and then combined to make a cortical and subcortical GM mask that was used in further analysis. This GM mask was utilized for CBF extraction within GM. We extracted mean CBF values from the CBF maps warped to MNI space obtained in Section 2.4.2 using the GM mask. CBF was also extracted from the CBF maps

Table 1
Participant Characteristics and Demographics.

	Control	TBI	p
N	35	29	–
Age (years)	35.2 (10.2)	32.1 (13.1)	0.303
Sex	25 M; 10F	19 M; 10F	0.568
Race	1 A; 1H; 12 W; 22 AA	1 A; 4H; 16 W; 8 AA	0.613
Average Education (years)	13.25 (2.17)	13.65 (2.50)	0.487
Post-Traumatic Amnesia (days)	–	22.7 (18.8)	–
Days To Follow Command	–	7.6 (11.5)	–
Glasgow Coma Scale	–	9.8 (3.6)$^{+}$	–
Time Post-Injury (days)	–	Time Point: 1: 100.1 (18.5)2: 184.2 (18.1)3: 366.9 (21.7)	–
Mechanism of Injury	–	Vehicle: 22 Fall: 5 Assault: 2	–

Mean (STD); M = Male; F = Female; A = Asian; H = Hispanic; W = White; AA = African American. $^{+}$This number is based on 19 subjects; the remaining subjects were intubated (3) and sedated (7). $^{-}$ Vehicle accidents include motor vehicle accidents, automobile versus pedestrian, automobile versus pedestrian/scooter, and motorcycle/bicycle.

obtained in Sections 2.5.1 and 2.5.2 using binarized *meta*-ROIs (described below).

2.4.4. Estimation of Regional Cortical Atrophy

To explore if any differences found in perfusion over the first year post-injury were due to structural changes as opposed to functional, we aimed to control any observed CBF change over time for regional change in volume. To estimate the regional atrophy, we calculated the regional Jacobian determinant between time points by utilizing ANTS (version 2.4.2). (Tustison, et al., 2018; Tustison, et al., 2013) This pipeline utilizes a subject specific template representing the midpoint of all T1 structural images between time points. (Avants et al., 2010) Voxel-wise maps of the Jacobian determinant were created using the diffeomorphic registration fields from the template building step by using the tool 'createJacobianDeterminantImage'. Specifically, the warps used during the registration of the structural volumetric cortical thickness map templates across time points were combined to create log-transformed Jacobian maps from 3 to 12 months post-injury, 3 to 6 months post-injury, and 6 to 12 months post-injury. The resulting positive log-transformed Jacobian values indicate tissue expansion and the negative log-transformed Jacobian values indicate tissue contraction. Additional processing considerations for focal lesions frequently encountered in TBI are accomplished via cost-function masking, (Kim et al., 2010; Ripollés et al., 2012) which was used to reduce the influence of focal lesions on cortical volume estimation.

2.5. Statistical Analyses.

2.5.1. Cerebral Blood Flow in traumatic Brain injury and Healthy controls

To characterize CBF in TBI patients in the first year following injury, we compared both GM and regional CBF in patients at 3, 6 and 12 months post-injury with healthy controls (HC).

GM CBF. To compare GM CBF in TBI and HC, we conducted a one-way ANOVA and post hoc tests corrected for multiple comparisons (Tukey's honestly significant difference test) in SPSS (IBM) using the extracted CBF values from the GM mask (Section 2.4.3). Neuroimaging results are displayed using MRIcron (brains in radiological convention) and charts and figures are displayed using Jupyter Notebook (Kluyver and Ragan-Kelley, 2016) (e.g., seaborn, matplotlib; Python 3 http://www.python.org).

Regional CBF. We conducted voxel-wise independent samples t-tests controlled for family-wise error ($p < .001$) and cluster size ($k = 100$) implemented for the comparison of the CBF levels between HC and TBI participants at 3, 6, and 12 months post-injury. A cluster extent-based (k) thresholding for family wise error (FWE) rate of the *p*-value was employed using a Gaussian random-field method implemented by SPM12. This analysis was aimed to elucidate the direction of regional CBF alterations in TBI as compared to HC at each time point. Significant clusters from voxel-wise independent t-tests were labeled using the peak coordinates. The voxel-wise independent t-tests resulted in clusters with a maximum of 3 peak coordinates 8 mm apart. Regions of interest (ROIs) containing clusters of significantly altered CBF were then labeled using Harvard Oxford Cortical and Subcortical Structural Atlas (FSL). (Desikan et al., 2006) The labels with the highest GM probabilities are reported. If the peak value could not be labeled using the Harvard Oxford Atlas (e.g., cerebellum), we manually determined where the peak coordinate resides and deemed the region as 'Outside of Atlas.'.

2.5.2. Cerebral Blood Flow change over time in traumatic Brain injury

To characterize temporal changes in hypoperfusion in TBI patients, we compared both GM and regional CBF in patients with TBI at 3, 6 and 12 months post-injury using within-subject designs.

GM CBF. To compare longitudinal GM CBF in TBI patients at 3, 6, and 12 months post-injury, we conducted a repeated measures analysis of variance (ANOVA) test using the extracted CBF values from the GM mask (Section 2.4.3).

Regional CBF. We examined the whole brain longitudinal changes of CBF within TBI patients using voxel-wise paired samples t-tests controlled for family-wise error ($p < .005$) and cluster size ($k = 200$), between 3 and 6 months post-injury, 6 and 12 months post-injury, and 3 and 12 months post-injury. The same labeling mechanism was used as above.

Meta-ROI Definition. The level of hypoperfusion was calculated from the mean CBF within "*meta*-ROIs." The "*meta*-ROIs" were comprised of single ROIs that exhibited statistically significant differences in CBF between TBI patients at 3 and 6 months post-injury determined through voxel-wise paired *t*-test analysis. Mean CBF from the binarized *meta*-ROI mask was extracted. Since only one ROI was found when conducting the voxel-wise paired t-tests between patients with TBI at 6 and 12 months post-injury, the one ROI was binarized and the mean CBF was extracted for further analysis. In conclusion, there were two *meta*-ROIs used for analysis: 1) ROIs derived from significant differences in CBF between TBI patients at 3 and 6 months post-injury and 2) ROIs derived from significant differences in CBF between TBI patients at 6 and 12 months post-injury. We have used the same method in our previous work (Ware et al., 2017).

Correlational Analysis of CBF Changes and Neuropsychological Performance. The relationship between longitudinal changes in CBF and neuropsychological scores were assessed using partial Spearman's correlation coefficient by controlling baseline score/perfusion level, age, and education level and correcting for multiple comparisons (i.e., Bonferroni). Please note that all previous and remaining analyses are parametric tests due to the normal distribution of the data as determined by Shapiro-Wilk test. However, the neuropsychological data being correlated with CBF changes are not normally distributed, calling for non-parametric correlation testing.

When examining the relationship of the magnitude of change of mean GM CBF (derived from group-level analyses) with the magnitude of change in neuropsychological performance, we did not find any significant relationships (see Section 3.4). Since we are studying a patient group expected to exhibit heterogeneity in spatial patterns of injury, we used an individualized measure to capture the extent of the CBF reduction in each TBI patient, which was then used for correlational analysis. The extent of reduced CBF is measured as the volume of hypoperfused voxels determined through the individual-specific analysis using the distribution corrected z score (DisCo-Z) method. (Mayer et al., 2014) In short, we used this method to make subject-specific hypoperfusion maps in both the control and TBI groups. Each individual's CBF map is initially Z-transformed using voxel-wise mean and standard deviation of the control population. Z-thresholds for the control and subject populations are then cluster corrected based on data smoothness and corrected to eliminate bias resulting from varying degrees of freedom and non-independence of control subject responses with respect to reference mean and standard deviation. (Mayer et al., 2014; Watts et al., 2014).

2.5.3. Relationship between regional CBF and cortical atrophy in traumatic Brain injury

Following the procedure described in Section 2.4.4, voxel-wise log-transformed Jacobian maps were masked using the *meta*-ROIs determined from the longitudinal comparisons between time points within the TBI patient group. Using Marsbar, mean Jacobian values and mean CBF values were extracted in a 5 mm radius sphere with the center set as the most significant peak value within each of the clusters listed in Tables 6 and 7. We used repeated measures analysis of covariance (ANCOVA) to determine the change in CBF from 3 to 6 months post-injury and 6 to 12 months post-injury while covarying for change in Jacobian metric within the respective time frames.

3. Results

3.1. Characteristics of participants

Demographics, injury severity, clinical characteristics, and more details of TBI and control groups are listed in Table 1. This cohort is a sub-group of a larger sample that was included in our recent publication. (Ware et al., 2020) There were no significant demographic differences between TBI and HC groups. Participants with TBI were characterized as moderate-severe as defined by the characteristics in Table 1. Focal lesions are mainly located in the frontal and temporal lobes (Fig. 1). There is minimal overlap between focal lesions and regions of reduced CBF.

3.2. Reduced CBF in traumatic Brain injury patients at 3, 6, and 12 months Post-Injury

GM CBF. Mean GM CBF values at each time point (HC: 44.76 ml/100 g/min; TBI 3 months post-injury: 40.23; 6 months post-injury: 37.19; 12 months post-injury: 37.77 ml/100 g/min) were lower in the TBI group compared to HC (Fig. 2). One-way ANOVA demonstrated a significant group difference ($F(3,118) = 3.589$, $p = 0.016$, $n_p^2 = 0.084$). Post hoc comparisons corrected for multiple comparisons revealed a significant difference in GM CBF between HC and patients with TBI at 6 ($p = 0.021$; Fig. 2) and patients with TBI at 12 months post-injury ($p = .045$). However, there was not a significant difference in GM CBF between HC and patients with TBI at 3 months post-injury ($p = .310$).

Regional CBF. In voxel-wise analysis, we found widespread regions of significant hypoperfusion ($p < 0.001$, $k = 100$; Fig. 3, Tables 2, 3 and 4) in the TBI group at 3, 6, and 12 months post-injury compared to the HC. These regions included both cortical and subcortical areas as reported previously at 3 months post-injury. (Ware et al., 2020) The right anterior cingulum and left cerebellum were two regions that at 3 months post-injury displayed hypoperfusion in the TBI group compared to HC (Table 2). These two peaks within the significant clusters of hypoperfusion also showed decrease in CBF compared to controls at 6 and 12 months post-injury (Tables 3 and 4).

3.3. CBF change over time in traumatic Brain injury Patients.

GM CBF. From 3 to 12 months post-injury, we did not find a significant main effect of time post-injury on CBF levels of TBI patients in GM ($F(2,56) = 2.164$, $p = .124$, $n_p^2 = 0.072$; Fig. 2).

Regional CBF. Through voxel-wise analysis, we found a worsening of hypoperfusion among the TBI group with multiple areas exhibiting a decrease in CBF from 3 to 12 months post-injury ($p < .005$, $k = 200$) and 3 to 6 months post-injury ($p < .005$, $k = 200$). Areas of CBF decrease from 3 to 12 months post-injury and 3 to 6 months post-injury are listed in Tables 4 and 5. Most of the worsening of hypoperfusion is concentrated from 3 to 6 months post-injury. CBF was also significantly lower

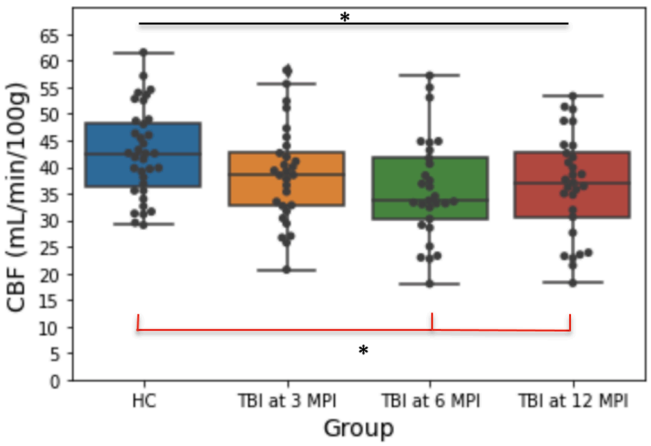

Fig. 2. Mean Gray Matter Cerebral Blood Flow in 35 Healthy Controls and 29 Traumatic Brain Injury Patients at 3, 6, and 12 Months Post-Injury. Black line indicates results from One-Way ANOVA. Red line indicates results Tukey's Honestly Significant Difference Test.* $p < .05$.

at 12 months post-injury compared to 3 months post-injury at multiple regions including, right Heschl's gyrus, left central opercular cortex, left supramarginal gyrus, right putamen, right caudate, left precuneus, right cuneus, and left caudate (Table 5). In contrast, there were no regions with significant decreases in CBF between 6 and 12 month post-injury (Table 7). However, there was an increase in CBF in the right precuneus from 6 to 12 months post-injury ($p < .005$, $k = 200$; Figs. 2 and 3).

Using ANTS (Section 2.5.3), we calculated and then extracted log-transformed Jacobian values within the areas showing CBF changes between time points (e.g., 3 to 6 months post-injury, 6 to 12 months post-injury). We aimed to determine if the observed CBF change was related to atrophy during the same time interval. Change in CBF in the sphere around peak coordinates remained significant while covarying for the Jacobian determinant within the same sphere across all peak coordinates (Supplemental Table 2).

3.4. Relationship between change of Cerebral Blood Flow and neuropsychological score changes

Using results from the voxel-wise paired t-tests comparing HC and TBI patients at 3, 6, and 12 months post-injury, we created meta-ROIs (Section 2.5.2). We correlated the change of mean CBF values from the (meta-)ROI with the change of neuropsychological domain scores across time points (i.e., 3–6 months post-injury and 6–12 months post-injury). After multiple comparison correction (for the number of neuropsychological domains) and including age, baseline (CBF level or

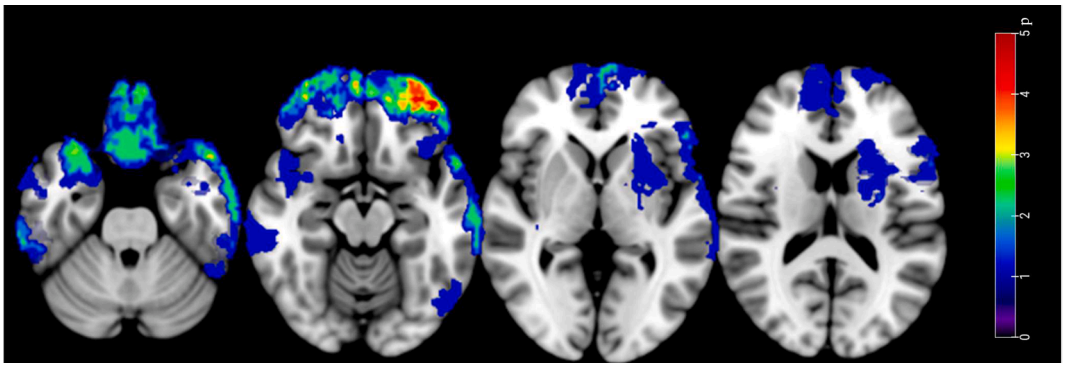

Fig. 1. Lesion Frequency Overlap Map in Patients with Focal Lesions (N = 22). Frequency is defined as the number of patients (p) displaying a lesion in the given area (0 to 5pt).

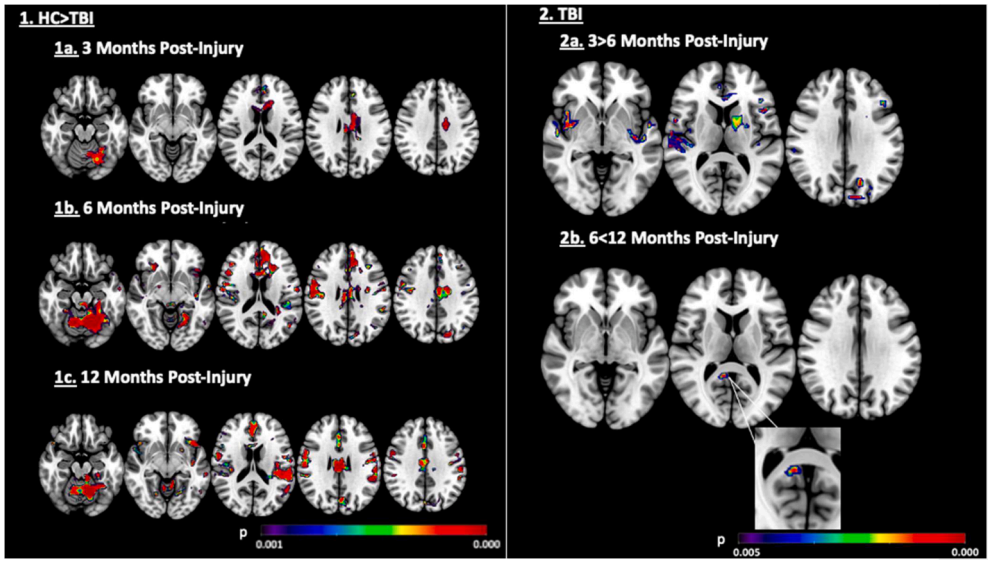

Fig. 3. Patterns of Cerebral Blood Flow 1. Between Group Difference in CBF in HC and TBI at 3 (1a), 6 (1b), and 12 (1c) Months Post-Injury ($p < .001$, $k = 100$) and 2. Longitudinal Within Group Difference in CBF in TBI from 3 to 6 (2a) and 6 to 12 (2b) Months Post-Injury ($p < .005$, $k = 200$).

Table 2
Areas of Hypoperfusion in Traumatic Brain Injury Patients at 3 Months Post-Injury Compared to Healthy Controls.

Location	Peak Coordinates (mm)	t	k	FWE p (cluster level)
a.Anterior Cingulate Gyrus	−6–4 28	4.87	1334	0.000
a. Left Cerebral White Matter	−16–12 34			
a.Right Posterior/Anterior Cingulate Gyrus	−4–18 24			
b.Outside of Atlas; Left Cerebellum	−8–60 −18	4.61	1030	0.000
b.Outside of Atlas; Left Cerebellum	−26–60 −18			
b.Outside of Atlas; Left Cerebellum	−24–70 −18			
c. Cingulate Gyrus/ Paracingulate Gyrus	4 42 18	3.96	318	0.006
c.Right Paracingulate Gyrus/Anterior Cingulate Cortex	−6 38 22			
c.Right Paracingulate Gyrus	−14 36 22			

Peak coordinates of local maxima are reported per each cluster (maximum 3 maxima) in mm. Cluster sizes (k) are reported in voxels. P value is reported at the level of significance for the cluster corrected for family wise error.

neuropsychological score), and education covariates, these relationships did not reach statistical significance.

The relationship between longitudinal CBF change with longitudinal behavioral change was better described using an individual-specific analysis (DisCo-Z; Section 2.5.2). Please refer to Supplemental Table 3 for a summary of correlations between CBF and behavior from the study cohort. Individual-specific analysis revealed heterogeneity in the trajectory of CBF changes from 3 to 12 months post-injury with some patients improving in the extent of hypoperfusion while others did not improve. Overall, there was a general trend of an increasing extent of hypoperfusion from 3 to 6 months post-injury. Using partial Spearman correlation and controlling for age, baseline (CBF level or neuropsychological score), and education level, we found that the extent of hypoperfusion difference from 3 to 6 months post-injury was correlated with change of EF from 3 to 6 months post-injury (rho = -0.436, p =.026; not corrected for multiple comparisons). In other words, a smaller change in the extent of hypoperfusion (less hypoperfusion) was correlated with a greater improvement in EF from 3 to 6 months post-injury. This extent of hypoperfusion difference from 3 to 6 months post-injury, however, was not correlated with change of PS from 3 to 6 months post-injury (rho = -0.266, p =.190) or with change of VL from 3 to 6 months post-injury (rho = -0.218, p =.285). Additionally, there was no significant correlation between change in the extent of hypoperfusion from 6 to 12 months post-injury with change in EF (rho = 0.322, p =.088), PS (rho = 0.171, p =.375), and VL (rho = 0.052, p =.789) from 6 to 12 months post-injury.

4. Discussion

4.1. CBF in traumatic Brain injury patients during the first year Post-Injury compared to Healthy controls

Using ASL MRI, our study is the first to delineate the temporal pattern of CBF alternations in patients with chronic msTBI at 3, 6, and 12 months post-injury. We observed regional hypoperfusion in both hemispheres in the TBI group compared to HC. This is consistent with previous literature demonstrating GM hypoperfusion in chronic msTBI. (Ware et al., 2020; Amyot et al., 2018) GM CBF reduction in TBI patients was present at each of the studied time points and was more pronounced in TBI at 6 months post-injury as compared to 3 and 12 months post-injury, suggesting that microvascular injury or dysfunction may worsen over time in the early chronic post-injury period with potential recovery. Regions of hypoperfusion included both cortical and subcortical areas in accordance with previous findings (Ware et al., 2020; Kim et al., 2010; Amyot et al., 2018) (Tables 2, 3, and 4). The right anterior cingulum and left cerebellum were two regions that displayed hypoperfusion in the TBI group at 3 months post-injury compared to HC. These two regions also showed hypoperfusion compared to HC at 6 and 12 months post-injury. A previous study examined amyloid plaque density in chronic msTBI patients (between 11 and 17 years post-injury). (Scott et al., 2016) The study found that there was an increased C-Pittsburgh compound B binding potential within the cingulate cortex (posterior) and cerebellum in TBI compared to controls and patients with Alzheimer's disease using positron emission tomography imaging. There was a positive correlation between time post-injury and C-Pittsburgh compound B binding potential within the posterior cingulate cortex, suggesting that there is a plaque accumulation in these areas over time. Studies focusing on brain connectivity in msTBI further implicate these regions as vulnerable to both structural and functional

Table 3
Areas of Hypoperfusion in Traumatic Brain Injury Patients at 6 Months Post-Injury Compared to Healthy Controls.

Location	Peak Coordinates (mm)	t	k	FWE p (cluster level)
a.Outside of Atlas; Left Cerebellum	−14–60 −18	6.54	4721	0.000
a.Outside of Atlas; Left Cerebellum	−20–52 −22			
a.Parahippocampal Gyrus	−20–38 −24			
b.Left Insular Cortex	−40 18–6	5.15	1006	0.000
b.Left Temporal Pole	−46 18–28			
b.Left Frontal Pole	−40 40 24			
c.Left Superior Lateral Occipital Cortex/Cuneus	−18–78 36	5.10	226	0.029
c.Left Cuneus Cortex	−10–80 26			
c.Left Cuneus Cortex	−2–82 28			
d.Right Postcentral Gyrus	52–12 28	5.06	2224	0.000
d.Right Insular Cortex	34–12 10			
d.Right Precentral Gyrus	54 4 30			
e.Left Cerebral White Matter	−20 26 20	4.97	4446	0.000
e.Left Paracingulate Gyrus	−8 36 26			
e.Left Anterior Cingulum	0 42 14			
f.Right Frontal Orbital Cortex	22 28–10	4.93	1327	0.000
f.Right Frontal Pole	44 40 2			
f.Right Inferior Frontal Gyrus	50 16 14			
g.Left Postcentral Gyrus/ Central Opercular Cortex	−60–10 14	4.82	220	0.032
g.Left Postcentral Gyrus	−56–8 24			
g.Left Postcentral Gyrus	−44–12 26			
h.Left Supracalcarine Cortex	−18–64 12	4.78	684	0.000
h.Left Lingual Gyrus	2–76 4			
h.Left Precuneus Cortex	−14–54 6			
i.Left Central Opercular Cortex/Planum Polare	−56 0 2	4.74	1917	0.000
i.Left Middle Temporal Gyrus	−54–60 −4			
i.Left Insular Cortex	−34–24 4			
j.Right Angular Gyrus	54–48 16	4.60	262	0.016
j.Right Parietal Operculum Cortex	50–34 32			
j.Right Middle Temporal Gyrus	60–46 10			
k.Posterior Cingulate Gyrus	2–44 16	3.74	396	0.002
k.Right Precuneus Cortex	14–58 12			
k.Right Precuneus Cortex	22–58 18			

Peak coordinates of local maxima are reported per each cluster (maximum 3 maxima) in mm. Cluster sizes (k) are reported in voxels. P value is reported at the level of significance for the cluster corrected for family wise error.

Table 4
Areas of Hypoperfusion in Traumatic Brain Injury Patients at 12 Months Post-Injury Compared to Healthy Controls.

Location	Peak Coordinates (mm)	t	k	FWE p (cluster level)
a.Left Parietal Operculum Cortex/Supramarginal Gyrus	−56–38 28	5.68	4247	0.000
a.Left Middle Temporal Gyrus	−54–60 −4			
a.Left Middle Temporal Gyrus	−52–58 10			
b.Outside of Atlas; Left Cerebellum	−14–58 −18	5.50	2462	0.000
b.Brain Stem	−8–36 −20			
b.Left Temporal Occipital Fusiform Cortex	−30–48 −22			
c.Left Anterior/Posterior Cingulate Gyrus	−4–16 26	5.30	1058	0.000
c.Right Posterior Cingulate Gyrus	4–18 26			
c.Right Juxtapositional Lobule Cortex	10–2 60			
d.Right Precentral Gyrus	54 4 32	4.64	3016	0.000
d.Right Frontal Pole	48 36 6			
d.Right Postcentral Gyrus	56–18 28			
e.Right Precentral Gyrus	42–14 44	4.59	193	0.048
e.Right Precentral Gyrus/ Postcentral Gyrus	40–22 54			
e.Right Precentral Gyrus	30–22 56			
f.Left Superior Lateral Occipital Cortex	−16–86 30	4.21	340	0.004
f.Left Precuneus Cortex	−4–72 26			
f.Left Superior Lateral Occipital Cortex	−18–76 38			
g.Right Caudate	10 12 12	4.13	1220	0.000
g.Right Anterior Cingulate Gyrus	4 42 18			
g.Right Anterior Cingulate Gyrus	2 6 44			

Peak coordinates of local maxima are reported per each cluster (maximum 3 maxima) in mm. Cluster sizes (k) are reported in voxels. P value is reported at the level of significance for the cluster corrected for family wise error.

connectivity disruptions, which may be related to cognitive deficits. (Hayes et al., 2016; Merkley et al., 2013; Scheibel et al., 2007; Hillary, 2015) Future studies should further investigate these two regions and their relationship with microvascular dysfunction over time post-injury in msTBI patients. Overall, reductions in GM CBF were observed primarily between 3 and 6 months post-injury, implicating this early chronic time frame as a period of potential vulnerability to progressive microvascular pathology warranting more detailed examination.

4.2. Temporal dynamics of hypoperfusion in traumatic Brain injury patients at 3, 6, and 12 months Post-Injury

Cross-sectional studies from our group examining CBF in chronic msTBI patients have shown global decreases in CBF between from time points ranging from 3 to 330.2 months post-injury, (Ware et al., 2020; Kim et al., 2010) which aligns with the results from our current study. The current study builds upon these results by shedding light on the time course of post-TBI CBF alterations and how they vary across TBI patients. Using a well-characterized cohort with similar assessment time points post-injury, we demonstrated that multiple brain regions show a progressive decrease in CBF from 3 to 6 months post-injury, while there is a stabilization of CBF from 6 to 12 months post-injury. This implicates the 3 to 6 months post-injury time period as a potentially important window in the evolution of microvascular injury after TBI necessitating more detailed investigation particularly with regards to interventions targeting microvascular dysfunction.

Post-TBI CBF reductions have previously been demonstrated to occur in the absence of and independent from visible structural damage, (Kim et al., 2010; Haber, 2018) and may persist for years after injury. (DeWitt and Prough, 2003) Even though CBF changes occur independent of focal lesions, it is possible that more subtle atrophy that detectable quantitatively (yet not radiologically) can confound reduced CBF by partial volume effects. (Petr et al., 2018) In our cohort, the change of CBF from 3 to 12 months post-injury was not related to cortical atrophy. This suggests that observed CBF reductions in our cohort reflect reductions in perfusion rather than the confounding effects of atrophy. These findings open the floor for future research examining post-TBI CBF reductions beyond 1 year post-injury.

4.3. Stabilization of hypoperfusion at 6 months Post-Injury and the role of the precuneus

While decreasing CBF was seen in TBI patients between 3 and 6 months post-injury, no further reduction of CBF was observed from 6 to 12 months post-injury. This suggests a relative stabilization of CBF after 6 month post-injury in TBI patients as a group. Interestingly, there was

Table 5
Areas of Decreasing Cerebral Blood Flow in Traumatic Brain Injury Patients From 3 to 12 Months Post-Injury.

Location	Peak Coordinates (mm)	t	k	FWE p (cluster level)
a.Right Central Opercular Cortex/Heschl's Gyrus	54–16 10	5.42	896	0.000
a.Right Planum Polare/ Temporal Pole	56 6–2			
a.Right Heschl's Gyrus	40–20 8			
b.Left Central Opercular Cortex	−60–20 16	5.21	1258	0.000
b.Left Parietal Operculum Cortex	−62–36 22			
b.Left Supramarginal Gyrus	−64–44 10			
c.Right Putamen	22 8 8	4.26	238	0.000
c.Right Caudate	10 12 8			
c.Right Lateral Ventricle	12–16 20			
d.Left Precuneus	0–72 42	4.07	224	0.000
d.Right Cuneus	4–78 36			
d.Left Superior Lateral Occipital Cortex/ Precuneus	−12–74 46			
e.Left Cerebral White Matter	−20–2 14	3.91	503	0.000
e.Left Caudate	−10–2 16			
e.Left Cerebral White Matter	–22 0–8			

Peak coordinates of local maxima are reported per each cluster (maximum 3 maxima) in mm. Cluster sizes (k) are reported in voxels. P value is reported at the level of significance for the cluster corrected for family wise error.

Table 6
Areas of Decreasing Cerebral Blood Flow in Traumatic Brain Injury Patients From 3 to 6 Months Post-Injury.

Location	Peak Coordinates (mm)	t	k	FWE p (cluster level)
a.Left Cuneus Cortex	−8–84 28	5.14	396	0.000
a.Left Supracalcarine Cortex	–22–62 20			
a.Left Superior Lateral Occipital Cortex	−20–80 34			
b.Right Central Opercular Cortex	58–10 16	4.59	1452	0.000
b.Right Central Opercular Cortex	48–14 12			
b.Right Parietal Operculum Cortex	60–24 16			
c.Left Inferior Frontal Gyrus	−46 16 12	4.09	743	0.000
c.Left Cerebral White Matter	–22 12 20			
c.Left Middle Frontal Gyrus	−46 20 26			
d.Left Planum Polare/ Medial Temporal Gyrus	−44–18 −12	3.96	388	0.000
d.Left Insular Cortex	−36–16 −2			
d.Left Planum Polare	−52–2 −6			
e.Left Anterior Cingulate Cortex	−2 30 6	3.84	259	0.000
e.Left Cerebral White Matter	−12 34 8			
e.Right Anterior Cingulate Gyrus	4 42 10			

Peak coordinates of local maxima are reported per each cluster (maximum 3 maxima) in mm. Cluster sizes (k) are reported in voxels. P value is reported at the level of significance for the cluster corrected for family wise error.

an increase in CBF from 6 to 12 months post-injury observed in the right precuneus. The precuneus has been implicated as a key region of the default mode network (DMN) (Utevsky et al., 2014) and involved in highly integrated tasks, (Cavanna and Trimble, 2006) as well as a factor

Table 7
Areas of Increase in Cerebral Blood Flow in Traumatic Brain Injury Patients From 6 to 12 Months Post-Injury.

Location	Peak Coordinates (mm)	t	k	FWE p (cluster level)
a.Right Cerebral White Matter	32–52 22	4.27	250	0.000
a.Right Precuneus	10–46 10			
a.Right Precuneus/ Supracalcarine Cortex	26–54 16			

Peak coordinates of local maxima are reported per each cluster (maximum 3 maxima) in mm. Cluster sizes (k) are reported in voxels. P value is reported at the level of significance for the cluster corrected for family wise error.

in the development of Alzheimer's disease and subsequent neurodegeneration (Yokoi et al., 2018; Karas et al., 2007; Klaassens et al., 2017) and an indicator of the severity of cognitive impairment. (Thomas et al., 2019; Ikonomovic et al., 2011; Wierenga et al., 2014; Hayashi et al., 2020; Zhang et al., 2021; Duan et al., 2020) Previous research supports the role of the precuneus in cognition, memory, and attention. (Cavanna and Trimble, 2006) In this study, the peak coordinates of the ROI that include the right precuneus appear to be located within the ventral subdivision, which is specifically associated with the DMN. (Zhang and Li, 2012) This is supported by earlier work in the rhesus monkey demonstrating that the ventral precuneus is anatomically connected with the dorsolateral prefrontal cortex, the inferior parietal lobule, and the superior temporal sulcus. (Zhang and Li, 2012; Morecraft et al., 2004; Pandya and Seltzer, 1982) The precuneus generally has been shown to be the first hypoperfused region in dementia patients and Alzheimer's disease, (Miners et al., 2016) as early as 10 years before dementia development. (Love and Miners, 2016) Post-mortem tissue from patients with early Alzheimer's disease has shown hypoperfusion and reduced oxygenation in the precuneus. (Miners et al., 2016).

In TBI, we have previously found that the right precuneus was hypoperfused in 27 msTBI patients compared to 22 HC also during resting state in the chronic stage (range: 4.1 to 330.2 months post-injury) in addition to global CBF reductions. (Kim et al., 2010) The precuneus has also been previously found to display altered resting-state functional connectivity with other nodes within the DMN in msTBI patients at varying times post-injury and to predict cognitive impairment. (Hillary, 2015; Bonnelle et al., 2011; Hillary, 2011; Sharp and Ham, 2011; Palacios, 2013) One study (Soman, 2014) found that glucose metabolism decreased in the right precuneus and left angular gyrus with increasing TBI severity. While observing the Jacobian metrics of the precuneus *meta*-ROI, we did not find that the atrophy affected the change in CBF of the precuneus from 6 to 12 months post-injury. This suggests that the CBF increase from 6 to 12 months post-injury in the precuneus is independent from structural changes and may be a compensatory mechanism. This calls for further investigation in the subcortical connections with the precuneus, the subdivisions of the precuneus, and its blood supply, especially given the functional role of the precuneus and its implications in neurodegeneration.

4.4. Behavioral correlations with Cerebral Blood Flow

CBF has been found to be frequently associated with cognition and neurological outcome in TBI and other populations. (Benedictus, 2017; Olm et al., 2016; Sweeney et al., 2018; Xekardaki et al., 2015) The current study builds upon these results by investigating relationships between CBF and neuropsychological trajectories, but more specifically executive function, verbal learning, and processing speed. Among our cohort, we have previously demonstrated that CBF at 3 months post-injury in TBI patients predicted processing speed improvement from 3 to 12 months post-injury. (Ware et al., 2020) The current study builds upon these results by investigating relationships between longitudinal

changes in CBF and neuropsychological trajectories. Despite detectable longitudinal CBF changes within the TBI patients, no significant correlations were observed with changes in neuropsychological performance from 3 to 6 and 6 to 12 months post-injury using a voxel-wise, group-level analysis approach. This lack of relationship may owe to limitations in sensitivity of this analysis approach which inherently relies upon a consistent spatial distribution of CBF alterations across individuals, which is unlikely to occur in patients with TBI. The lack of relationship may also highlight the heterogeneity of TBI and the heterogeneity of the recovery process, more generally. In Supplemental Fig. 1, the heterogeneity of the direction and magnitude of change in the 6 to 12 months post-injury meta-ROI is displayed. Although using voxel-wise, group-level analysis determines a significant increase in this region in TBI patients from 6 to 12 months post-injury, there is variability within the TBI group, which may be attributed to the lack of significant relationship between this *meta*-ROI and neuropsychological performance.

We employed an individual-specific analysis to determine the extent of hypoperfusion and then correlated the change in hypoperfusion with the change in neuropsychological scores during the first year post-injury. We found a weak relationship seen between extent of hypoperfusion change from 3 to 6 months post-injury and EF from 3 to 6 months post-injury, when controlled for age, baseline (CBF level or neuropsychological score, respectfully), and education level. In other words, as the extent of hypoperfusion increased, the smaller the improvements in EF were seen (i.e., more hypoperfusion, worse EF). This implicates the magnitude of change from 3 to 6 months post-injury as an important time point that reflects change in cognitive change in one domain. Although this finding is tentative due to the statistical significance not being multiple comparison corrected, it supports our previously discussed finding; 3 to 6 months post-injury is a critical time period for the evolution of microvascular function after TBI. Future research should complement these findings by investigating longitudinal changes in CBF and more measures of cognitive function, psychological factors, and other neuropsychiatric measures.

Individual-specific analysis can yield complementary information to group-level analysis, especially for a patient group with known heterogeneity in neural damage and dynamic recovery trajectories. It is important to highlight the heterogeneity of TBI and that while TBI can share commonalities and hallmarks, individualized patient care is necessary and deserves more attention. Previous reports have supported the use of individual-specific analysis in the TBI population, which have shown to be more sensitive than group-level analyses. (Ware et al., 2017; Mayer et al., 2014) It was previously found that individual-specific analysis of diffusion tensor imaging metrics better detected patients with TBI who showed impaired processing speed compared to group-level analysis. (Ware et al., 2017) Our findings are similar in nature, where we found some relationship with behavior using individual-specific analysis while there was none using group-level analysis. However, this finding is tentative and should be replicated in a larger cohort. In addition, it may be the initial injury that is more strongly related to the amount of behavioral improvement than progressive damage (i.e., CBF). Future research should focus on disentangling ongoing degeneration related to initial injury that is either behaviorally or not behaviorally relevant.

4.5. Strengths and Limitations.

A strength of this study is the controlled and well-characterized nature of the TBI cohort which was enrolled longitudinally with little variation in follow up times (Table 1). Additionally, our sample is screened for msTBI with diffuse injuries through the inclusion/exclusion criteria which further increases the homogeneity. However, the sample size was small and from a monocentric urban center. Hence, this may limit the generalizability of our findings to the larger TBI population encompassing a much wider range of severities, and to those with larger focal lesions. The small sample size also may have affected the power and effect sizes of our results. In addition, localizing hypoperfusion is likely sample-specific and this can be influenced by the cohort and the heterogeneity of TBI. The recruitment process lacked screening for unipolar depressive disorders. We only screened for bipolar disorders in the TBI and HC cohorts, as it is unlikely that we would recruit participants with unipolar depression. Future studies should consider screening for both bipolar and unipolar disorders as to not confound participant recruitment. An inherent confound to our analysis is the structure of data collection: one time point measured for HC and three time points measured for TBI patients. Another limitation of the study was that the entire bilateral cerebellum was not included in the ASL scans. The region of the left cerebellum that was imaged was a region that revealed consistent significant hypoperfusion at each time point. Future studies should fully image the cerebellum to determine hypoperfusion in chronic TBI patients because of its potential contribution to chronic TBI impairment.

Lastly, there were some limitations with our analysis and imaging acquisition parameters, such as the use of 2D PCASL with non-background suppression. The sequence employed, however, has been successfully used in multiple studies. (Ware et al., 2020; Dolui et al., 2016; Xie et al., 2016; Dolui et al., 2020) The post-labeling delay (PLD) is also shorter than the recommended 1.8 s, (Alsop et al., 2015) but the slices are acquired sequentially from inferior to superior direction resulting in a PLD range of 1.5–2.3 s for the slices. Moreover, these are relatively young participants, and we did not observe any transit time artifacts.

4.6. Conclusions

Overall, we conclude that patients with msTBI exhibit widespread hypoperfusion which increases in magnitude and extent from 3 months to 1 year post-injury, with most of the decline in CBF occurring between 3 and 6 months post-injury. Potential treatments to halt or slow down the progression of CBF decline during the early chronic phase post-injury include noninvasive neuromodulation therapies, including transcranial photobiomodulation, (Hamblin, 2018) and pharmacologic vascular therapies, including Sildenafil. (Kenney, 2018; Sheng, 2017) Longitudinal CBF reductions in TBI patients are not explained by cortical atrophy during the first year post-injury. These longitudinal CBF reductions may not only be due to microvascular injury, but also due to diffuse microstructural damage. More research is needed to determine the causality. Subject-specific CBF analysis demonstrated an inverse correlation between the change in extent of hypoperfusion between 3 and 6 months post-injury with recovery in executive function over the same time period, suggesting short-term functional relevance of CBF measures. Overall, these results point to evolution, and in some cases progression, of microvascular dysfunction in the early chronic post-TBI period. In addition, this work suggests the early chronic functional relevance of CBF in msTBI, highlights the importance of monitoring progression of CBF reductions in patient care, and supports ASL MRI holding clinical utility for TBI patient care. Future studies will be needed to assess the longer-term implications of these perfusion abnormalities.

CRediT authorship contribution statement

Naomi L. Gaggi: Conceptualization, Methodology, Writing – original draft, Writing – review & editing. **Jeffrey B. Ware:** Writing – original draft, Conceptualization, Methodology, Writing – review & editing. **Sudipto Dolui:** Conceptualization, Methodology, Writing – review & editing. **Daniel Brennan:** Methodology. **Julia Torrellas:** Methodology. **Ze Wang:** Conceptualization, Methodology. **John Whyte:** Conceptualization, Writing – review & editing, Funding acquisition. **Ramon Diaz-Arrastia:** Conceptualization, Writing – review & editing. **Junghoon J. Kim:** Conceptualization, Methodology, Writing – original draft, Writing – review & editing, Funding acquisition, Supervision.

Declaration of Competing Interest

The authors declare that they have no known competing financial interests or personal relationships that could have appeared to influence the work reported in this paper.

Data availability

Data will be made available on request with a formal sharing agreement to protect patient privacy.

Acknowledgements

This research was supported by the NIH grants NINDS R01NS065980 (PI: JJK) and NINDS R01NS125408 (PI: JBW).

Author Disclosure Statement: No competing financial disclosures exist.

References

Alsop, D. C. *et al.* Recommended Implementation of Arterial Spin Labeled Perfusion MRI for Clinical Applications: A consensus of the ISMRM Perfusion Study Group and the European Consortium for ASL in Dementia. 36 (2015). doi:10.1002/mrm.25197.

Amyot, F., Kenney, K., Moore, C., Haber, M., Turtzo, L.C., Shenouda, C., Silverman, E., Gong, Y., Qu, B.-X., Harburg, L., Lu, H.Y., Wassermann, E.M., Diaz-Arrastia, R., 2018. Imaging of cerebrovascular function in chronic traumatic brain injury. J. Neurotrauma 35 (10), 1116–1123.

Avants, B.B., Yushkevich, P., Pluta, J., Minkoff, D., Korczykowski, M., Detre, J., Gee, J.C., 2010. The optimal template effect in hippocampus studies of diseased populations. NeuroImage 49 (3), 2457–2466.

Benedictus, M.R., et al., 2017. Lower cerebral blood flow is associated with faster cognitive decline in Alzheimer's disease. Eur. Radiol. 27, 1169–1175. https://doi.org/10.1007/s00330-01604450-z.

Bonnelle, V., Leech, R., Kinnunen, K.M., Ham, T.E., Beckmann, C.F., De Boissezon, X., Greenwood, R.J., Sharp, D.J., 2011. Default Mode Network Connectivity Predicts Sustained Attention Deficits after Traumatic Brain Injury. J. Neurosci. 31 (38), 13442–13451.

Bouma, G.J., Muizelaar, J.P., Choi, S.C., Newlon, P.G., Young, H.F., 1991. Cerebral circulation and metabolism after severe traumatic brain injury: the elusive role of ischemia. J. Neurosurg. 75, 685–693. https://doi.org/10.3171/jns.1991.75.5.0685.

Bouma, G.J., Muizelaar, J.P., Stringer, W.A., Choi, S.C., Fatouros, P., Young, H.F., 1992. Ultra-early evaluation of regional cerebral blood flow in severely head-injured patients using xenon-enhanced computerized tomography. J Neurosurg 77 (3), 360–368.

Brett, M., Anton, J.-L., Valabregue, R. & Poline, J.-B. Region of interest analysis using an SPM toolbox. in vol. 16 497 (8th international conference on functional mapping of the human brain, 2002).

Cavanna, A.E., Trimble, M.R., 2006. The precuneus: a review of its functional anatomy and behavioural correlates. Brain 129, 564–583. https://doi.org/10.1093/brain/awl004.

Chao, L.L., Buckley, S.T., Kornak, J., Schuff, N., Madison, C., Yaffe, K., Miller, B.L., Kramer, J.H., Weiner, M.W., 2010. ASL Perfusion MRI Predicts Cognitive Decline and Conversion From MCI to Dementia. Alzheimer Dis. Assoc. Disord. 24 (1), 19–27.

Desikan, R.S., Ségonne, F., Fischl, B., Quinn, B.T., Dickerson, B.C., Blacker, D., Buckner, R.L., Dale, A.M., Maguire, R.P., Hyman, B.T., Albert, M.S., Killiany, R.J., 2006. An automated labeling system for subdividing the human cerebral cortex on MRI scans into gyral based regions of interest. NeuroImage 31 (3), 968–980.

DeWitt, D.S., Prough, D.S., 2003. Traumatic cerebral vascular injury: The effects of concussive brain injury on the cerebral vasculature. J. Neurotrauma 20, 795–825. https://doi.org/10.1089/089771503322385755.

Ding, K., Tarumi, T., Tomoto, T., Mccolloster, M., Le, T., Dieppa, M., Diaz-Arrastia, R., Bell, K., Madden, C., Cullum, C.M., Zhang, R., 2020. Impaired cerebral blood flow regulation in chronic traumatic brain injury. Brain Res. 1743, 146924.

Dolui, S., Wang, Z.e., Wang, D.JJ., Mattay, R., Finkel, M., Elliott, M., Desiderio, L., Inglis, B., Mueller, B., Stafford, R.B., Launer, L.J., Jacobs, D.R., Bryan, R.N., Detre, J. A., 2016. Comparison of non-invasive MRI measurements of cerebral blood flow in a large multisite cohort. J. Cereb. Blood Flow Metab. 36 (7), 1244–1256.

Dolui, S., Li, Z., Nasrallah, I.M., Detre, J.A., Wolk, D.A., 2020. Arterial spin labeling versus 18F-FDG-PET to identify mild cognitive impairment. NeuroImage Clin. 25, 102146 https://doi.org/10.1016/j.nicl.2019.102146.

Duan, W., Sehrawat, P., Balachandrasekaran, A., Bhumkar, A.B., Boraste, P.B., Becker, J. T., Kuller, L.H., Lopez, O.L., Gach, H.M., Dai, W., 2020. Cerebral Blood Flow Is Associated with Diagnostic Class and Cognitive Decline in Alzheimer's Disease. J. Alzheimers Dis. 76 (3), 1103–1120.

Fonov, V., Evans, A., McKinstry, R., Almli, C., Collins, D., 2009. Unbiased nonlinear average age-appropriate brain templates from birth to adulthood. NeuroImage 47, S102. https://doi.org/10.1016/S1053-8119(09)70884-5.

Fonov, V., Evans, A.C., Botteron, K., Almli, C.R., McKinstry, R.C., Collins, D.L., 2011. Unbiased average age-appropriate atlases for pediatric studies. NeuroImage 54 (1), 313–327.

Haber, M., et al., 2018. Vascular abnormalities within normal appearing tissue in chronic traumatic brain injury. J. Neurotrauma 35, 2250–2258. https://doi.org/10.1089/neu.2018.56.84.

Hamblin, M.R., 2018. Photobiomodulation for traumatic brain injury and stroke. J. Neurosci. Res. 96, 731–743. https://doi.org/10.1002/jnr.24190.

Hayashi, H., Kobayashi, R., Kawakatsu, S., Morioka, D., Otani, K., 2020. Utility of Easy Z-Score Imaging System-Assisted SPECT in Detecting Onset Age-Dependent Decreases in Cerebral Blood Flow in the Posterior Cingulate Cortex, Precuneus, and Parietal Lobe in Alzheimer's Disease with Amyloid Accumulation. Dement. Geriatr. Cogn. Disord. Extra 10, 63–68. https://doi.org/10.1159/000507654.

Hayes, J.P., Bigler, E.D., Verfaellie, M., 2016. Traumatic brain injury as a disorder of brain connectivity. J. Int. Neuropsychol. Soc. 22, 120–137.

Hillary, F.G., et al., 2011. Changes in resting connectivity during recovery from severe traumatic brain injury. Int. J. Psychophysiol. 82, 115–123. https://doi.org/10.0116/j.ijpsycho.2011.03.011.

Hillary, F.G., et al., 2015. Hyperconnectivity is a fundamental response to neurological disruption. Neuropsychology 29, 59–75. https://doi.org/10.1037/neu000110.

Hlatky, R., Contant, C. F., Diaz-Marchan, P., B.Valadka, A. & Robertson, C. S. Significance of a Reduced Cerebral Blood Flow During the First 12 Hours After Traumatic Brain Injury. *Neurocrit. Care* **1**, 69–84 (2004). doi:10.1385/NCC:1:1:69.

Ikonomovic, M.D., Klunk, W.E., Abrahamson, E.E., Wuu, J., Mathis, C.A., Scheff, S.W., Mufson, E.J., DeKosky, S.T., 2011. Precuneus amyloid burden is associated with reduced cholinergic activity in Alzheimer disease. Neurology 77 (1), 39–47.

Inoue, Y., Shiozaki, T., Tasaki, O., Hayakata, T., Ikegawa, H., Yoshiya, K., Fujinaka, T., Tanaka, H., Shimazu, T., Sugimoto, H., 2005. Changes in Cerebral Blood Flow from the Acute to the Chronic Phase of Severe Head Injury. J. Neurotrauma 22 (12), 1411–1418.

Jackson, W.T., Novack, T.A., Dowler, R.N., 1998. Effective serial measurement of cognitive orientation in rehabilitation: The orientation log. Arch. Phys. Med. Rehabil. 79, 718–721. https://doi.org/10.1016/s0003-9993(98)90051-x.

Karas, G., Scheltens, P., Rombouts, S., van Schijndel, R., Klein, M., Jones, B., van der Flier, W., Vrenken, H., Barkhof, F., 2007. Precuneus atrophy in early-onset Alzheimer's disease: a morphometric structural MRI study. Neuroradiology 49 (12), 967–976.

Kenney, K., et al., 2018. Phosphodiesterase-5 inhibition potentiates cerebrovascular reactivity in chronic traumatic brain injury. Ann. Clin. Transl. Neurol. 5, 418–428.

Kenney, K., Amyot, F., Haber, M., Pronger, A., Bogoslovsky, T., Moore, C., Diaz-Arrastia, R., 2016. Cerebral Vascular Injury in Traumatic Brain Injury. Exp. Neurol. 275, 353–366.

Kim, J., Whyte, J., Patel, S., Avants, B., Europa, E., Wang, J., Slattery, J., Gee, J.C., Coslett, H.B., Detre, J.A., 2010. Resting Cerebral Blood Flow Alterations in Chronic Traumatic Brain Injury: An Arterial Spin Labeling Perfusion fMRI Study. J. Neurotrauma 27 (8), 1399–1411.

Kim, J., Whyte, J., Patel, S., Europa, E., Slattery, J., Coslett, H.B., Detre, J.A., 2012. A perfusion fMRI study of the neural correlates of sustained-attention and working-memory deficits in chronic traumatic brain injury. Neurorehabil. Neural Repair 26 (7), 870–880.

Klaassens, B.L., van Gerven, J.M.A., van der Grond, J., de Vos, F., Möller, C., Rombouts, S.A.R.B., 2017. Diminished Posterior Precuneus Connectivity with the Default Mode Network Differentiates Normal Aging from Alzheimer's Disease. Front. Aging Neurosci. 9 https://doi.org/10.3389/fnagi.2017.00097.

Kluyver, T., Ragan-Kelley, B., Fernando P'erez, Granger, B., Bussonnier, M., Frederic, J., … Willing, C. (2016). Jupyter Notebooks – a publishing format for reproducible computational workflows. In F. Loizides & B. Schmidt (Eds.), *Positioning and Power in Academic Publishing: Players, Agents and Agendas* (pp. 87–90).

Love, S., Miners, J.S., 2016. Cerebrovascular disease in ageing and Alzheimer's disease. Acta Neuropathol. (Berl.) 131, 645–658. https://doi.org/10.1007/s00401-015-1522-0.

Marion, D.W., Darby, J., Yonas, H., 1991. Acute regional cerebral blood flow changes caused by severe head injuries. J. Neurosurg. 74, 407–414. https://doi.org/10.3171/jns.1991.74.3.0407.

Martin, N.A., Patwardhan, R.V., Alexander, M.J., Africk, C.Z., Lee, J.H., Shalmon, E., Hovda, D.A., Becker, D.P., 1997. Characterization of cerebral hemodynamic phases following severe head trauma: hypoperfusion, hyperemia, and vasospasm. J Neurosurg 87 (1), 9–19.

Mayer, A.R., Bedrick, E.J., Ling, J.M., Toulouse, T., Dodd, A., 2014. Methods for identifying subject-specific abnormalities in neuroimaging data: Subject-Specific Abnormalities in Neuroimaging. Hum. Brain Mapp. 35, 5457–5470. https://doi.org/10.1002/hbm.22563.

Merkley, T.L., Larson, M.J., Bigler, E.D., Good, D.A., Perlstein, W.M., 2013. Structural and Functional Changes of the Cingulate Gyrus following Traumatic Brain Injury: Relation to Attention and Executive Skills. J. Int. Neuropsychol. Soc. 19, 899–910.

Miners, J.S., Palmer, J.C., Love, S., 2016. Pathophysiology of Hypoperfusion of the Precuneus in Early Alzheimer's Disease: Hypoperfusion of Precuneus in Alzheimer's Disease. Brain Pathol. 26, 533–541. https://doi.org/10.1111/bpa.12331.

Morales, D.M., Marklund, N., Lebold, D., Thompson, H.J., Pitkanen, A., Maxwell, W.L., Longhi, L., Laurer, H., Maegele, M., Neugebauer, E., Graham, D.I., Stocchetti, N., McIntosh, T.K., 2005. Experimental models of traumatic brain injury: Do we really need to build a better mousetrap? Neuroscience 136 (4), 971–989.

Morecraft, R.J., Cipolloni, P.B., Stilwell-Morecraft, K.S., Gedney, M.T., Pandya, D.N., 2004. Cytoarchitecture and cortical connections of the posterior cingulate and adjacent somatosensory fields in the rhesus monkey. J. Comp. Neurol. 469, 37–69.

Obrist, W.D., Gennarelli, T.A., Segawa, H., Dolinskas, C.A., Langfitt, T.W., 1979. Relation of cerebral blood flow to neurological status and outcome in head-injured patients. J. Neurosurg. 51 (3), 292–300.

Olm, C.A., Kandel, B.M., Avants, B.B., Detre, J.A., Gee, J.C., Grossman, M., McMillan, C. T., 2016. Arterial spin labeling perfusion predicts longitudinal decline in semantic variant primary progressive aphasia. J. Neurol. 263 (10), 1927–1938.

Palacios, E. M. *et al.* Resting-State Functional Magnetic Resonance Imaging Activity and Connectivity and Cognitive Outcome in Traumatic Brain Injury. *JAMA Neurol.* **70**, 845 (2013). doi:10.001/jamaneurol.2013.38.

Pandya, D.N., Seltzer, B., 1982. Intrinsic connections and architectonics of posterior parietal cortex in the rhesus monkey. J. Comp. Neurol. 204, 196–210.

Patenaude, B., Smith, S.M., Kennedy, D.N., Jenkinson, M., 2011. A Bayesian model of shape and appearance for subcortical brain segmentation. NeuroImage 56, 907–922. https://doi.org/10.1016/j.neuroimage.2011.02.046.

Petr, J., Mutsaerts, H.J.M.M., De Vita, E., Steketee, R.M.E., Smits, M., Nederveen, A.J., Hofheinz, F., van den Hoff, J., Asllani, I., 2018. Effects of systematic partial volume errors on the estimation of gray matter cerebral blood flow with arterial spin labeling MRI. Magn. Reson. Mater. Phys. Biol. Med. 31 (6), 725–734.

Rabinowitz, A.R., Hart, T., Whyte, J., Kim, J., 2018. Neuropsychological recovery trajectories in moderate to severe traumatic brain injury: Influence of patient characteristics and diffuse axonal injury – Erratum. J. Int. Neuropsychol. Soc. 24 (3), 237–246.

Ramos-Cejudo, J., Wisniewski, T., Marmar, C., Zetterberg, H., Blennow, K., de Leon, M. J., Fossati, S., 2018. Traumatic brain injury and Alzheimer's disease: The cerebrovascular link. EBioMedicine 28, 21–30.

Ripollés, P., Marco-Pallarés, J., de Diego-Balaguer, R., Miró, J., Falip, M., Juncadella, M., Rubio, F., Rodriguez-Fornells, A., 2012. Analysis of automated methods for spatial normalization of lesioned brains. NeuroImage 60 (2), 1296–1306.

Sandsmark, D.K., Bashir, A., Wellington, C.L., Diaz-Arrastia, R., 2019. Cerebral Microvascular Injury: A Potentially Treatable Endophenotype of Traumatic Brain Injury-Induced Neurodegeneration. Neuron 103, 367–379. https://doi.org/10.1016/j.neuron.2019.06.002.

Scheibel, R.S., Newsome, M.R., Steinberg, J.L., Pearson, D.A., Rauch, R.A., Mao, H., Troyanskaya, M., Sharma, R.G., Levin, H.S., 2007. Altered Brain Activation During Cognitive Control in Patients With Moderate to Severe Traumatic Brain Injury. Neurorehabil. Neural Repair 21 (1), 36–45.

Scott, G., Ramlackhansingh, A.F., Edison, P., Hellyer, P., Cole, J., Veronese, M., Leech, R., Greenwood, R.J., Turkheimer, F.E., Gentleman, S.M., Heckemann, R.A., Matthews, P.M., Brooks, D.J., Sharp, D.J., 2016. Amyloid pathology and axonal injury after brain trauma. Neurology 86 (9), 821–828.

Sharp, D.J., Ham, T.E., 2011. Investigating white matter injury after mild traumatic brain injury. Curr. Opin. Neurol. 24, 558–563.

Sheng, M., et al., 2017. Sildenafil Improves Vascular and Metabolic Function in Patients with Alzheimer's Disease. J. Alzheimers Dis. 60, 1351–1364.

Shively, S., Scher, A.I., Perl, D.P., Diaz-Arrastia, R., 2012. Dementia resulting from traumatic brain injury: What is the pathology? Arch. Neurol. 69, 1245–1251. https://doi.org/10.1001/archneurol.2011.3747.

Smith, S.M., Jenkinson, M., Woolrich, M.W., Beckmann, C.F., Behrens, T.E.J., Johansen-Berg, H., Bannister, P.R., De Luca, M., Drobnjak, I., Flitney, D.E., Niazy, R.K., Saunders, J., Vickers, J., Zhang, Y., De Stefano, N., Brady, J.M., Matthews, P.M., 2004. Advances in functional and structural MR image analysis and implementation as FSL. NeuroImage 23, S208–S219.

Soman, S., et al., 2014. Mid Life Hypometabolism In The Precuneus May Be Associated With Prior History Of Traumatic Brain Injury (TBI) (P5.329). Neurology 82, P5.329.

Soustiel, J.F., Glenn, T.C., Shik, V., Boscardin, J., Mahamid, E., Zaaroor, M., 2005. Monitoring of Cerebral Blood Flow and Metabolism in Traumatic Brain Injury. J. Neurotrauma 22 (9), 955–965.

Stamatakis, E.A., Wilson, J.T.L., Hadley, D.M., Wyper, D.J., 2009. SPECT Imaging in Head Injury Interpreted with Statistical Parametric Mapping, p. 8. https://doi.org/10.1089/neu.2009.1215.

Sweeney, M.D., Kisler, K., Montagne, A., Toga, A.W., Zlokovic, B.V., 2018. The role of brain vasculature in neurodegenerative disorders. Nat. Neurosci. 21, 1318–1331. https://doi.org/10.1038/s41593-018-0234-x.

Telischak, N.A., Detre, J.A., Zaharchuk, G., 2015. Arterial spin labeling MRI: Clinical applications in the brain. J. Magn. Reson. Imaging 41, 1165–1180. https://doi.org/10.1002/jmri.24751.

Thomas, B., Sheelakumari, R., Kannath, S., Sarma, S. & Menon, R. N. Regional Cerebral Blood Flow in the Posterior Cingulate and Precuneus and the Entorhinal Cortical Atrophy Score Differentiate Mild Cognitive Impairment and Dementia Due to Alzheimer Disease. *Am. J. Neuroradiol.* ajnr;ajnr.A6219v1 (2019) doi:10.3174/ajnr.A6219.

Tustison, N. J. *et al.* The ANTs cortical thickness processing pipeline. in (eds. Weaver, J. B. & Molthen, R. C.) 86720K (2013). doi:10.1117/12.2007128.

Tustison, N. J. *et al.* The ANTs longitudinal cortical thickness pipeline. *bioRxiv* 1–43 (2018).

Utevsky, A.V., Smith, D.V., Huettel, S.A., 2014. Precuneus Is a Functional Core of the Default-Mode Network. J. Neurosci. 34, 932–940. https://doi.org/10.1523/JNEUROSCI.4227-13.2014.

Wang, Z.e., Aguirre, G.K., Rao, H., Wang, J., Fernández-Seara, M.A., Childress, A.R., Detre, J.A., 2008. Empirical optimization of ASL data analysis using an ASL data processing toolbox: ASLtbx. Magn. Reson. Imaging 26 (2), 261–269.

Ware, J.B., Hart, T., Whyte, J., Rabinowitz, A., Detre, J.A., Kim, J., 2017. Inter-subject variability of axonal injury in diffuse traumatic brain injury. J. Neurotrauma 34 (14), 2243–2253.

Ware, J.B., Dolui, S., Duda, J., Gaggi, N., Choi, R., Detre, J., Whyte, J., Diaz-Arrastia, R., Kim, J.J., 2020. Relationship of Cerebral Blood Flow to Cognitive Function and Recovery in Early Chronic Traumatic Brain Injury. J. Neurotrauma 37 (20), 2180–2187.

Watts, R., Thomas, A., Filippi, C.G., Nickerson, J.P., Freeman, K., 2014. Potholes and Molehills: Bias in the Diagnostic Performance of Diffusion-Tensor Imaging in Concussion. Radiology 272, 217–223. https://doi.org/10.1148/radiol.14131856.

Wierenga, C.E., Hays, C.C., Zlatar, Z.Z., de la Torre, J.C., 2014. Cerebral Blood Flow Measured by Arterial Spin Labeling MRI as a Preclinical Marker of Alzheimer's Disease. J. Alzheimers Dis. 42 (s4), S411–S419.

Wilde, E.A., Wanner, I.-B., Kenney, K., Gill, J., Stone, J.R., Disner, S., Schnakers, C., Meyer, R., Prager, E.M., Haas, M., Jeromin, A., 2022. A Framework to Advance Biomarker Development in the Diagnosis, Outcome Prediction, and Treatment of Traumatic Brain Injury. J. Neurotrauma 39 (7-8), 436–457.

Wilson, L., Stewart, W., Dams-O'Connor, K., Diaz-Arrastia, R., Horton, L., Menon, D.K., Polinder, S., 2017. The chronic and evolving neurological consequences of traumatic brain injury. Lancet Neurol. 16 (10), 813–825.

Xekardaki, A., Rodriguez, C., Montandon, M.-L., Toma, S., Tombeur, E., Herrmann, F.R., Zekry, D., Lovblad, K.-O., Barkhof, F., Giannakopoulos, P., Haller, S., 2015. Arterial Spin Labeling May Contribute to the Prediction of Cognitive Deterioration in Healthy Elderly Individuals. Radiology 274 (2), 490–499.

Xie, L., Dolui, S., Das, S.R., Stockbower, G.E., Daffner, M., Rao, H., Yushkevich, P.A., Detre, J.A., Wolk, D.A., 2016. A brain stress test: Cerebral perfusion during memory encoding in mild cognitive impairment. NeuroImage Clin. 11, 388–397.

Yokoi, T., Watanabe, H., Yamaguchi, H., Bagarinao, E., Masuda, M., Imai, K., Ogura, A., Ohdake, R., Kawabata, K., Hara, K., Riku, Y., Ishigaki, S., Katsuno, M., Miyao, S., Kato, K., Naganawa, S., Harada, R., Okamura, N., Yanai, K., Yoshida, M., Sobue, G., 2018. Involvement of the Precuneus/Posterior Cingulate Cortex Is Significant for the Development of Alzheimer's Disease: A PET (THK5351, PiB) and Resting fMRI Study. Front. Aging Neurosci. 10 https://doi.org/10.3389/fnagi.2018.00304.

Yushkevich, P.A., Piven, J., Hazlett, H.C., Smith, R.G., Ho, S., Gee, J.C., Gerig, G., 2006. User-guided 3D active contour segmentation of anatomical structures: Significantly improved efficiency and reliability. NeuroImage 31 (3), 1116–1128.

Zhang, Y., Brady, M., Smith, S., 2001. Segmentation of brain MR images through a hidden Markov random field model and the expectation-maximization algorithm. IEEE Trans. Med. Imaging 20, 45–57. https://doi.org/10.1109/42.906424.

Zhang, S., Li, C.-S., 2012. Functional connectivity mapping of the human precuneus by resting state fMRI. NeuroImage 59 (4), 3548–3562.

Zhang, Q., Wang, Q., He, C., Fan, D., Zhu, Y., Zang, F., Tan, C., Zhang, S., Shu, H., Zhang, Z., Feng, H., Wang, Z., Xie, C., 2021. Altered Regional Cerebral Blood Flow and Brain Function Across the Alzheimer's Disease Spectrum: A Potential Biomarker. Front. Aging Neurosci. 13, 630382 https://doi.org/10.3389/fnagi.2021.630382.